IEEE Access
Multidisciplinary | Rapid Review | Open Access Journal

Received November 9, 2020, accepted November 30, 2020, date of publication December 14, 2020,
date of current version December 30, 2020.

Digital Object Identifier 10.1109/ACCESS.2020.3044441

Demonstration of a 1 MJ XRAM Generator Supplying a Medium Caliber Railgun

OLIVER LIEBFRIED AND VOLKER BROMMER
French-German Research Institute of Saint-Louis (ISL), 68301 Saint-Louis, France

Corresponding author: Oliver Liebfried (oliver.liebfried@isl.eu)

This work was supported in part by the French Directorate General of Armaments (DGA) within the ANR Astrid program under Grant ANR-14-ASTR-0025.

ABSTRACT The electric power supply for an electromagnetic launcher has to provide energy in the mega-joule range within an acceleration time which only lasts for milliseconds. Today's giga-watt pulsed power generators are based on large capacitor banks and are therefore unsuitable for most mobile applications. Thus, power supply research focuses on size reduction by means of alternative technologies like inductive storage. The XRAM topology, where several inductors are charged in a series and discharged in a parallel connection, is a concept for inductive current multiplication. This technique requires simultaneous switching of closing and opening switches and was realized by using thyristors turned off by a counter-current pulse (inverse current commutation with semiconductor devices - ICCOS). At the French-German Research Institute of Saint-Louis (ISL), several aspects of this technology have been investigated and several demonstrators for different energies have been developed. Nowadays, the development of inductive pulsed power generators advances towards energy levels relevant for future applications. This paper presents the development of a 1 MJ XRAM generator which demonstrates the suitability of this technology by supplying the medium-caliber ISL railgun RAFIRA during dynamic experiments. The results of the latest experiment are reported, where the XRAM generator was charged to 842 kJ. A current of 40 kA was successfully interrupted by the ICCOS opening switches and an 80 g brush projectile was accelerated to 1120 m/s. The railgun current was switched off at the time of the projectile's bore-exit, thus approximating a rectangular current pulse shape. Experimental results are compared to outcomes achieved with capacitor banks as railgun power supply.

INDEX TERMS Pulsed power supplies, electromagnetic launching, railguns, power semiconductor switches, energy storage, inductors.

I. INTRODUCTION

Electromagnetic accelerators convert electrical energy into kinetic energy of a projectile and can outperform powder-actuated guns in several disciplines, e.g. precision, velocity, impact energy or safety (no explosives). Although the railgun is a topic with a long research history, it currently receives a lot of attention worldwide [1]. This was triggered by the efforts of the U.S. Navy to develop a long-range artillery railgun with a kinetic energy of 32 MJ, which is now tested along the Potomac River at the Naval Surface Warfare Center in Dahlgreen and at the White Sands Missile Range in New Mexico [2]. Other countries intensified or started their own R&D of this technology because the railgun is seen as a ''true warfighter game changer'' as the U.S. Navy stated in [3]. Thus, it is not a surprise that photos and videos of a Chinese railgun turret mounted on a landing ship for sea testing were published online in 2018 [4]. Videos of railgun demonstrators performing media-effective demonstration shots were also publicly released by Turkish defense technology companies [5]. They show a demonstrator which is mounted in a turret and it is claimed that it is supplied by a 10 MJ electrical pulsed power supply (PPS).

For the French-German Research Institute of Saint-Louis (ISL), there are currently two conceivable military scenarios for the application of an electromagnetic railgun. One scenario corresponds to the U.S. Navy's scenario using the railgun to accelerate massive projectiles (of the order of 10 kg

The associate editor coordinating the review of this manuscript and approving it for publication was Firuz Zare.

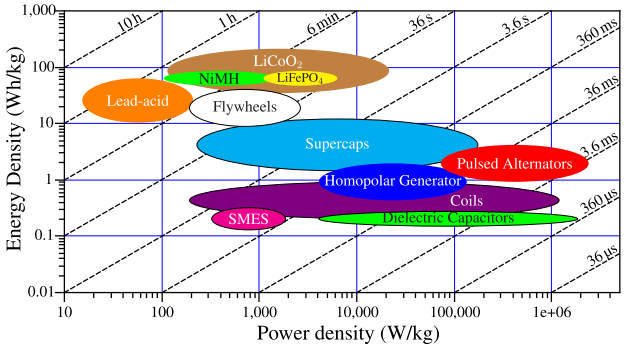

FIGURE 1. Ragone plot of various realized energy storages. Devices are considered without auxiliaries like switches, vacuum pumps, cooling systems,....

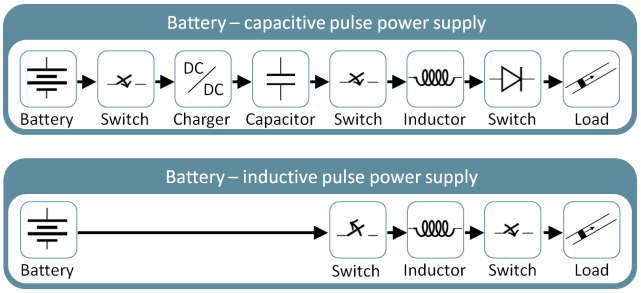

FIGURE 2. Energy conversion chain of a capacitive and an inductive pulsed power supply with a battery as prime energy source.

and more) to velocities of 2.5 km/s, thus reaching muzzle energies surpassing modern conventional ship and land artillery systems [6]. The second scenario is air-defense, where projectiles with a relatively low weight are fired in rapid succession as last line of defense against missiles or approaching aircrafts. For existing close-in weapon systems (CIWS), like ' Phalanx" or ' Goalkeeper', typical velocities are below 1500 m/s, while a railgun should be able to perform better [7]. No matter what the final application will look like, the size and the weight of the PPS is the key for a mobile application of the weapon system. In most cases, PPS based on capacitor energy storages are considered the most appropriate solution. It currently operates reliably at the appropriate energy level in railgun or high magnetic field facilities around the world. However, they are fixed installations and not suited for mobile applications. Here PPS based on inductive storage steps in. Inductive storage offers a higher energy density than capacitors (see Fig. 1) and a fast charging and discharging capability. In addition, they can be directly supplied by a primary energy source without the need of high voltage converters as in the case for capacitors. Thus, less conversion steps are needed within the energy conversion chain (see Fig. 2), which enables more compact systems [8].

The technical principle of inductive pulsed power generators has been known since the beginning of the railgun research. However, capacitive solutions were favored due to the complexity of opening switches which are required in inductive pulsed power supplies (IPPS). Since the beginning of this millennium, IPPS have increasingly been investigated. The focus of these studies was on current amplifying circuits which are seen as a possible solution to reduce the stress requirements of the opening switch. Inductive pulsed power circuits can be categorized in three basic topologies:

- Single coils
- XRAM generator
- Pulse transformer

The first is the traditional circuit with one coil, where the charging current is equal to the load current. In an XRAM generator, several coils are charged in a series connection and discharged in a parallel connection, thus, multiplying the current at the load by the number of stages under the condition of a small load inductance. The term XRAM is derived from the Marx generator, its capacitive counterpart (inverse spelling). Pulse transformer are making use of the energy conservation law: interrupting the small current of the primary windings of a transformer leads to a sudden current increase in the secondary windings in order to maintain the magnetic field which is stored within the transformer windings. Details of all three principles can be found in [9], [10].

A. EARLIER IPPS R&D

In the international context, several IPPS were developed or investigated. Projects in Australia and the USA already employed large single inductive storages, but they were used for voltage amplification in combination with large flywheels as energy source [11]–[13]. The biggest efforts were probably done by a research group at Soreq NRC, Israel, which was working for more than 10 years on this topic (see [14] and literature therein). They built an XRAM generator with GTO semiconductor switches at a maximum stored energy and a maximum output current of 25 kJ and 2.5 kA, respectively. With a single coil circuit, they reached 515 kJ of stored energy at a current of 64 kA in a jellyroll coil and transferred it to a resistive load. For this setup, an explosive circuit breaker was applied as opening switch.

Since 2000, several research groups, one in the USA, one in Japan and three in China built small scale demonstrators of IPPS for electromagnetic launcher.

In Japan, they built and tested a demonstrator which was very similar to an XRAM generator [15]. They achieved a 490 A peak output current by using lead acid batteries to charge each of 12 cryo-cooled coils individually. IGBT switches were used as opening switches. Based on the results, the Japanese researchers designed a generator with 800 superconducting coils in order to generate an output current of 2.5 MA. It is unknown if this design was ever realized and if the project is ongoing.

In the U.S., the so-called "STRETCH meat grinder" was built and tested [16]–[18]. The meat grinder belongs to the family of pulse transformers where a rapid current change in the primary windings results in a high secondary current. In this way, a current amplification of nearly 11 was achieved by interrupting the primary current with an IGCT opening

switch and a capacitor in a parallel connection for voltage limitation. The maximum charging current of 2 kA was amplified to an output current of 21 kA. The U.S. project was discontinued when the Institute of Advanced Technologies has been closed [19].

B. CURRENT IPPS R&D

Besides ISL, several research groups in China are currently working on IPPS. Three research groups can be distinguished by regular publications until now (2020).

Since several years, the R&D group of Xinjie Yu at the Tsinghua University in Beijing is working on the optimization of the meat grinder technology [10]. They developed several revisions of it and combined it with variants of the counter-current opening switch technology [10], [20]. The proposed circuits were proved by experimental laboratory setups with energies below 2 kJ. A milestone was the development of an 80-kJ prototype of a pulse-forming unit (PFU) based on the STRETCH meat grinder with SECT circuit topology [21]. This inductive PFU combines a cylindrical air-core transformer, a voltage protection capacitor, a control unit, cables and switches in a compact frame with a rectangular volume of 35 liters. The primary power supply was not integrated.

Pulsed power transformers (PPT) with high-temperature superconducting (HTS) primary and normal conducting secondary windings have been under development at the Chengdu Southwest Jiaotong University at least since 2012. Li *et al.* developed a one-stage HTSPPT prototype applying a short cylindrical coil with a maximum energy density of 70 kJ/m^3 (cryocooling equipment not considered) [22]. They were able to amplify the primary current of 100 A to 4.26 kA at a resistive load of 1 mΩ. In parallel, Wu *et al.* developed a prototype of an HTS transformer coil with a long cylindrical shape and a maximum energy density of 55 kJ/m^3. Three different topologies were tested with it: the classical pulse transformer, the meat grinder and the STRETCH meat grinder topology [23]–[25]. The best current amplification from 100 A to 4.29 kA was realized with the STRETCH meat grinder topology [25]. Subsequently, the short coil design of Li *et al.* was chosen, presumably because of the better coupling coefficient and the better suitability for a toroidal arrangement of multiple modules. Later publications from the Southwest Jiaotong University deal with simulations of the mutual inductance between several modules (toroidal arrangement) [26]–[28] or the asynchronous ignition of several modules (pulse shaping) [28]. The latter issue was experimentally tested with 2 HTSPPT modules which have been slightly modified since 2012 (smaller inductances but better coupling) [29].

In 2016, a research group at the Shandong University in Zibo, China, started publishing articles about the very same HTSPPT design. One of the authors, Haitao Li, was with the Chengdu Southwest Jiatong University before. Most publications are about simulations to investigate different system design aspects (i.e. circuit topology variations, pulse forming with several modules, matching of inductance to a railgun load). The HTSPPT was also simulated with ICCOS opening switches (ICCOS - inverse current commutation with semiconductor devices). The authors concluded that ICCOS enables the application of higher energies and that this technology is considerably cheaper than IGCTs [30], [31]. A small prototype for an inductive energy storage of 37 J was developed and used to demonstrate a repetitive operation with a frequency of 5 Hz at a current ratio of 1.11 kA to 92.5 A. Finally, Zhang *et al.* present a simulation based system design of multiple HTSPPT modules supplying a railgun [32]. In this work, the authors continued the concept of [33] and combined the HTSPPT with an XRAM topology: The primary windings of 12 HTSPPT modules are charged in series by a common power supply and the secondary windings are connected in parallel to the railgun. Thus, the authors predict that a feeding current of 2 kA could be amplified to 460 kA at an opening switch voltage of 19.5 kV. The 12 HTSPPT modules could be set-up in a toroidal arrangement with an outer radius of 0.57 m. Consequently, the SMES would have a cylindrical volume of 1.02 m^3 without the cooling apparatus for a temperature of 20 K, which means a net energy density of 4.4 MJ/m^3.

Until now, a mature IPPS is not available. However, many capacitor-based laboratory setups proved their reliability and therefore most users still prefer capacitors [34]. The advantage of a higher energy density of IPPS only becomes apparent in systems with high energy and has yet to be demonstrated.

C. EARLIER WORK AT ISL

At ISL, the development of compact pulsed power supplies started together with the beginning of the railgun research. A modular 50 kJ PFU, consisting of a capacitor, a pulse forming inductance, a semiconductor closing and crowbar switch assembly, was built in several versions and is one of the major achievements of the program [35]. It is successfully used in several laboratory setups and installations like the PEGASUS facility [36]. Since then, the size of capacitive PFUs could be constantly reduced. The latest type of the developed PFU utilizing a capacitor with an energy density of 1.82 MJ/m^3 features 1.2 MJ/m^3 (see Fig. 3). One major focus of this work was and still is the development of smaller and more powerful switches which are crucial for all kinds of pulsed power generators. Therefore, it is logical that, when the interest turned toward inductive PPSs, the researchers started with the research on semiconductor switches which can be applied as opening switches. Different kind of power semiconductor switches like MOSFETs, IGBTs and IGCTs were investigated in this respect [37], [38]. Finally, this led to the development of the so-called ICCOS switch [39]. The ICCOS is basically a fast switching thyristor with an additional circuit for the generation of a counter current in order to return them into the blocking state. The same technique was previously used at the TNO in Delft, the Netherlands, with a mechanical opening switch

FIGURE 3. Development steps of 50 kJ capacitive PFUs at ISL [48].

in the mega-ampere level [40]–[42]. In case of semiconductor switches, such current levels require devices in a parallel connection which is critical in terms of a reliable operation. The slightest switching difference of a single device can lead to a failure of the total switch. Increasing the switching power by connecting several devices in series is somehow less challenging. Thus, the XRAM topology is a solution to avoid or reduce parallel switches. The concept was introduced by Werner Koch at Marx' High Voltage Institute at Brunswick Technical University [43] and its operation principle is as follows: First, several inductors are energized in a series connection by a current source (battery, supercapacitors, rotating machines or other means). After the inductors are charged, they are connected to the load in a parallel connection by corresponding switches, subsequently producing an output current which is the sum of the individual inductor currents. The current amplification depends on the number of stages which defines the segmentation of components (inductor, switches,..).

The ICCOS was applied to a two-stage XRAM generator and it was found that it is well suited for this kind of IPPS. Subsequently, the number of stages was increased gradually. XRAM generators with 4, 8 and 20 stages were developed [44]–[46]. The 20-stage technology demonstrator was realized in a compact toroidal arrangement with the electronics placed in the vicinity of the coil [46]. It proved that synchronized switching of a multitude of stages can be realized with the ICCOS switch. Next, XRAM generators with a higher energy were developed and connected to real loads. A 4-stage XRAM was used to feed a wire explosion in order to investigate the effect of high-voltage peaks created during the plasma ignition [44]. Finally, a 4-stage XRAM generator was tested with a stored energy of up to 200 kJ with an output current of 40 kA in order to demonstrate that it can be used to supply a railgun [47]. The demonstration of a larger XRAM generator with an output current suitable for one of the railguns at ISL was a logical extension of this work. Consequently, the goal was a 1 MJ XRAM generator with an array of opening switch devices to interrupt a charging current of more than 40 kA.

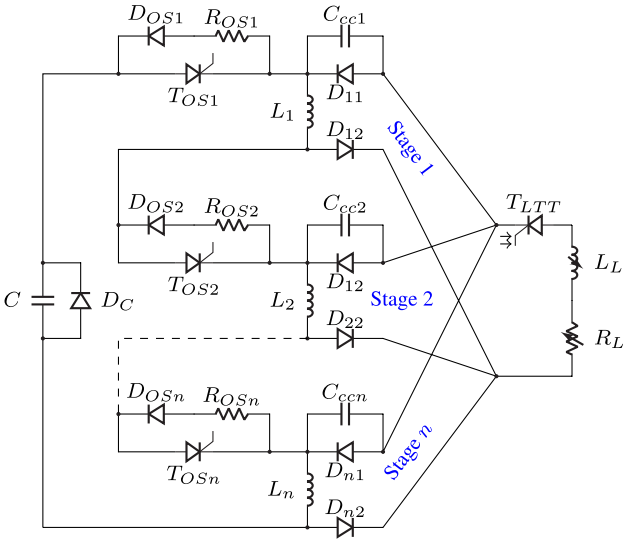

FIGURE 4. Schematic of the XRAM generator.

D. OPERATION PRINCIPLE

Although the switching requirements are influenced by the topology, the essential requirement for an inductive pulsed power generator is still an appropriate opening switch. In this respect, semiconductor switches offer clear advantages in terms of synchronous switching, maintenance costs, repetition rate and durability. Research on the use of different semiconductor switches in connection with inductive pulse power generation has been carried out in the past and is reported in [37] and [38]. In subsequent work, the ICCOS was developed for a current amplitude of 28 kA [39]. In [49], different active semiconductor opening switch concepts are compared to the ICCOS system. The ICCOS counter-current principle was chosen due to clear advantages in terms of low power dissipation, synchronous switching, compactness of the switch assemblies, and last but not least cost efficiency. The main features of the ICCOS will be described briefly in combination with a three stage XRAM generator circuit shown in Fig. 4. The circuit diagram is simplified with respect to the number of stages and details of the electronic circuit (i.e. neglected snubber elements). Since the operation principle is independent of the number of stages, only 3 stages are shown. The last one is separated from the rest by a dashed line to indicate the possibility of extension. Several inductors ($L_1 \ldots L_n$), which might or might not be coupled magnetically, are connected in a series connection via fast switching thyristors $T_{OS1} \ldots T_{OSn}$. The charging circuit is completed by the capacitor bank C. An intermediate energy storage like batteries, supercaps or a flywheel would be preferable for this purpose, but corresponding equipment with sufficient power is not available at ISL. Each inductor is individually connected to the load (L_L, R_L) via diodes ($D_{11} \ldots D_{n2}$). During the operation, the magnetic storage is charged by the power supply if $T_{OS1} \ldots T_{OSn}$ are switched on. The main switch T_{LTT} initiates the synchronous discharge to the load when the desired inductor current amplitude

is reached. At this moment, several processes happen at once: The pre-charged capacitors $C_{cc2} \dots C_{ccn}$ discharge via T_{OS}, the load and T_{LTT} with a short but high current pulse. The current within $T_{OS1} \dots T_{OSn}$ becomes negative until the charge carriers have been removed from the pn-junction. The remaining counter-current pulse is conducted by the diodes D_{OS} and resistance R_{OS}, which ensures a negative voltage at T_{OS} for the duration of the pulse and thus ensures the reliable turn-off of T_{OS} thyristors. The counter-current simultaneously establishes the current in the load. The current commutation from the charging to the discharging circuit completes with the end of the counter-current pulse. After this, the magnetic storage discharges into the load. This is necessary until the projectile leaves the bore at the muzzle. At this point, it is advantageous to stop the discharge in order to avoid a large plasma arc at the muzzle. Therefore, $T_{OS1} \dots T_{OSn}$ are switched on again before the projectile leaves the muzzle and the current commutates back to the charging circuit. The impedance of the plasma arc leads to a high muzzle voltage and supports a quick commutation. At this point, the coils could be recharged but for now, the power supply is bypassed by the diodes D_C and the energy is converted to heat within the circuit.

II. EXPERIMENTAL SETUP

Originally, the goal was an XRAM-generator with 20 stages on the basis of a toroidal coil with a total inductance of 1 mH and a DC-resistance of about 5 mΩ. A stored energy of 1 MJ was envisaged which requires a current of > 40 kA. Corresponding inductive storage and switch assemblies had to be developed to meet those goals.

A. TOROIDAL INDUCTIVE STORAGE

A toroidal inductive storage was built from 180 copper discs and an equivalent number of insulation discs. A D-shape design for homogeneous force distribution was approximated. The coil consists of 20 modules with individual connectors. Fig. 5 shows a photograph of the coil during assembly. Table 1 summarizes the measured specification of the coil. Its resistance changes according to

$$R_{coil} = 3.88\,\text{m}\Omega \cdot \sqrt{f} + 5\,\text{m}\Omega \tag{1}$$

with the frequency f due to skin effects. The coil was stress-tested by a pulsed current of up to 50 kA (1.25 MJ). Details on the coil's design, construction and testing were recently reported in [50].

B. SWITCHES

1) THE MAIN CLOSING SWITCH T_{LTT}

High power light triggered thyristors (LTTs) with a blocking voltage of 8 kV and pulse current capability of 90 kA for 10 ms have been chosen because they are available and robust while providing intrinsic galvanic separation at the gate [51]. Up to 8 LTT modules, which are usually applied in low inductive switching units for 50 kJ capacitive pulsed power

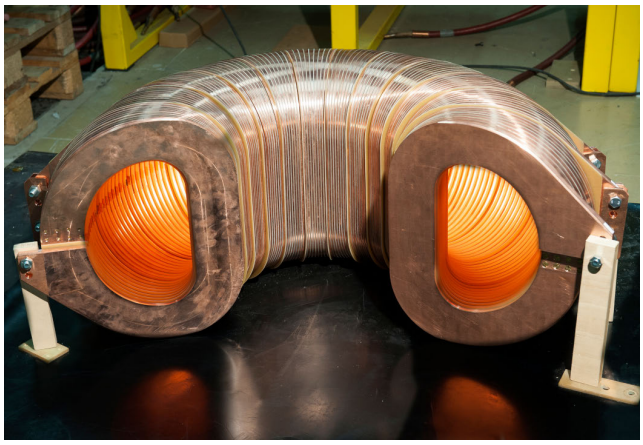

FIGURE 5. Unfinished toroidal inductive storage (12 of 20 modules).

TABLE 1. Measured coil specifications.

No. of segments	20
Outer diameter	960 mm
..with connectors	1030 mm
Inner diameter	260 mm
Height	423 mm
Volume	220 l
Weight	1050 kg
DC resistance	5 mΩ
Inductance @ 50 Hz	1 mH
Energy density @ 45 kA	4.5 MJ/m^3
Specific energy @ 45 kA	1 kJ/kg

modules, were applied in a parallel connection. Each switching module is connected with a separate high current coaxial cable. RC snubber circuits were adjusted to the circuitry during low energy experiments in order to protect the LTTs from high $\frac{dV}{dt}$ signals.

2) THE OPENING SWITCH T_{OS}

The use of semiconductor switches is limited by several parameters like voltage, max. current or the action integral $\int I^2 \text{dt}$, the $\frac{dI}{dt}$ or the $\frac{dV}{dt}$). The number of devices in a series connection is determined by the applied voltage. The number of devices in a parallel connection is determined by the current and the action integral. The synchronous switching of all switches is crucial for the save operation at high power levels. If only one device experiences a switching delay, single devices can be over-strained which can lead to an avalanche effect among the switch array. A homogeneous current distribution between parallelized switches is crucial but not easy to realize since manufacturing variations, different temperature coefficients and slight variations in the circuit design (i.e. resistance/inductance of wires) can cause asymmetries. Therefore, past XRAM generators were built with one thyristor stack per stage. In fact, it is one of the practical advantages of the XRAM circuitry in combination with the counter-current opening switch principle that the semiconductor devices can be switched in a series connection instead of a parallel connection. However, increasing the power without exceeding the current limit leads to several

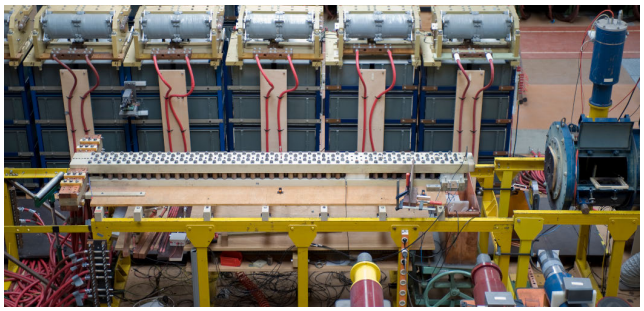

FIGURE 6. Railgun RAFIRA facility.

devices in parallel for the opening switches as well for the closing switches.

The theoretical design and size approximation for the ICCOS opening switch was described in [49]. The final semiconductor switch assemblies per stage consist of diode stacks with 3 diodes each ($D_{11} \ldots D_{n2}$) and one stack of 4 parallelized fast switching thyristors (T_{OS}). The latter are applied as opening switches according to the ICCOS principle. The symmetric current sharing between the devices was achieved by the introduction of mutual inductive coupling between the thyristor branches (see [52]).

Purpose-designed gate units with very little delay times (jitter) for the gate signals were developed and built for each stage. The gate unit is able to synchronously switch-on 8 thyristors. It is powered by long lasting Lithium batteries and receives the trigger signal by an optic fiber. Thus, the complete unit is galvanically separated from the control units. The temporal deviation of the gate signals was measured to be smaller than 100 ns. This satisfies our requirements for reliable synchronous switching. The gate signals are adjustable in pulse length and repetition rate, which is important for a second thyristor switch-on with respect to repetitive operation or muzzle arc prevention.

C. RAILGUN AND PROJECTILE

The railgun facility RAFIRA was chosen for experimental investigations because it has served for many experiments in the energy range around 1 MJ [53]. Thus, it allows us to compare experimental results with old recordings. The railgun has been built for repetitive shot investigations. In this case, however, recordings of single shot experiments were used for comparison. A photograph of the railgun can be seen in Fig. 6 and its specifications are given in Table 2. Note the open bore structure which allows easy access for in-bore investigations like X-ray pictures, velocity or magnetic field measurements [54]. Three X-ray tubes are placed in front of the railgun and one is mounted on top of the catch tank. They were used in the former experiments to investigate the projectile conditions but not during the XRAM generator experiments.

The standard brush projectiles of 80 grams were used for the experiments. The projectiles are made of a glass reinforced plastic (GRP) block and six copper brushes which are fixed in corresponding cut-outs (see Fig. 7). They are

TABLE 2. Parameters of railgun RAFIRA.

Length	3 m
Caliber	25 mm × 25 mm
Rail material	Dural
Rail cross section	25 mm × 20 mm
Inductance gradient	0.45 µH @ 100 kHz
Construction	GRP bars and steel bolts

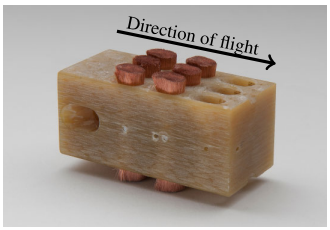

FIGURE 7. 80 g-projectile with 6 Cu-Cd brush armatures.

TABLE 3. Projectile specifications.

Length	55 mm
Width / height	24.5 mm
Mass	80.25 g
Brushes (CU)	6
Brush diameter	6 mm
Brush length	29 mm
Brush material	Cu-Cd
Sabot material	GRP

inserted at the breech before each shot. Its parameters are given in Table 3.

D. POWER SUPPLY

Railgun RAFIRA can be powered by up to 18 capacitor bank modules. Each 178 kJ-unit consists of 8 capacitors, a pulse forming inductance of 4 μH, a trigatron closing switch, 4 crowbar diode stacks and a corresponding charge/dump-panel. The backsides of some units are visible in in the background of the railgun in Fig. 6. The capacitors have an energy density of 0.3 MJ/m^3 and have reliably served their purpose for the last 30 years. Thirteen capacitor banks were used to charge the XRAM generator because a corresponding prime power supply with sufficient power was not available at the time of the experiments. The pulse forming inductances and switches of the capacitor banks were short-circuited for the duration of this test campaign.

E. ASSEMBLY

The XRAM-generator was assembled on a GRP insulating plate of 1.2 m × 1.2 m which was placed on a wooden structure for easy transportation by a forklift. Two sub-coils were connected in series in order to build a 10-stage XRAM-generator. Subsequently, ten semiconductor switch assemblies and three counter-current capacitors in parallel connection per stage were placed around the toroidal coil as shown in Fig. 8. Note, that the used capacitors are oversized but they were available in our lab. Therefore, their electrical specifications are not matched to the experimental circuit.

FIGURE 8. XRAM generator connected to the railgun RAFIRA.

TABLE 4. Characteristics of the 1 MJ XRAM generator.

XRAM stages	10
Max. magnetic energy	1 MJ
Total capacitance of C_{cc}	10.8 mF
Max. charge current	40 kA
Max. discharge current	400 kA
Opening switches	10 × 4 fast switching Thyristors
Main switch	8 LTTs
Inductance in charging mode	1 mH
Inductance in discharging mode	10 µH

All capacitors together could store an energy of 480 kJ but were only partially charged to 42 kJ during the latest experiment. The eight LTT switch units and the load were connected via 8 coaxial cables from the centered bus bar of the XRAM-generator. The main characteristics are summarized in Table 4.

F. METROLOGY

1) CURRENT MEASUREMENTS

Rogowski coils [55]–[57] are installed at each capacitor bank. They were developed to be installed at the current feeds and are connected to a passive filter and to the recording system inside a Faraday cage. The integration is performed by numerical computation [58], [59]. The error of these coils is below 1%. Furthermore, commercially available "clip-on" Rogowski coils [60] with an active integrator were used for the current measurements at the XRAM generator.

2) VOLTAGE MEASUREMENT

The voltage measurement between the rails of a railgun is regularly performed at the railgun's breech and muzzle. At ISL, the measurements are performed using voltage dividers, opto-electronic transmitters and oscilloscopes [59]. This measurement gives valuable information on the contact behavior between the armature and the rails. A sudden rise in voltage can be recognized if the armature leaves the railgun and if the current is not yet completely decayed. Then, a muzzle arc occurs which results in a high breech and muzzle voltage. The origin and meaning of the muzzle voltage were explained in [61], [62]. A commercial high voltage capacitive voltage divider [63] was used for the voltage measurements at the switches.

3) VELOCITY MEASUREMENT

The time-dependent position of the projectile was measured by B-dots located in vertically centered positions along the rails with distances of 98.5 cm, 22.5 cm and 4 cm, respectively, to the muzzle. The B-dots are loop sensors, also called search coils, with the active area being in plane with the side surface of the rails. Therefore, the magnetic field created by the current in the armature induces a voltage in a B-dot which changes its polarity when the armature passes the measurement position. The polarity change of the signal can be detected and is used for armature position detection. It allows to approximate the projectile velocity by assuming a linear acceleration between two measurement locations.

A Doppler radar at the breech was used during earlier experiments to record the velocity profile. Details of this system are given in [64].

G. IMPLEMENTATION OF THE EXPERIMENTS

Experimental testing started with low energy tests and a short-circuited railgun. With respect to the system impedance, the short-circuit at the railgun breech is equivalent to a projectile's armature at initial position. Thus, it was possible to test the setup and in particular the switches with respect to the new electrical circuit conditions. The counter-current circuit was adjusted to the new load and cable inductances. Several voltages and currents were monitored at different locations during repeated experiments in order to check for asymmetric current distributions between the thyristors and to avoid critical voltages.

Switching experiments with a short-circuited railgun were conducted until a charging-current of 28 kA (= railgun current of 280 kA). Up to this current, a very symmetric current sharing and a reliable switching behavior of the semiconductor components could be realized. Thus, further experiments were performed with a projectile instead of a short-circuit. In the following, the short-circuit was replaced by the brush projectile. A massive catch tank was installed for the interception of the projectiles (see the blue barrel on the right hand side in Fig. 6). The test campaign started with small energies which were stepwise increased. Subsequent railgun experiments were conducted with a stepwise increase of the capacitor charging voltage to 5 kV, 6 kV and 7 kV. At the last experiment, the charging voltage is close to the 7.5 kV-voltage limit of the used LTT switches.

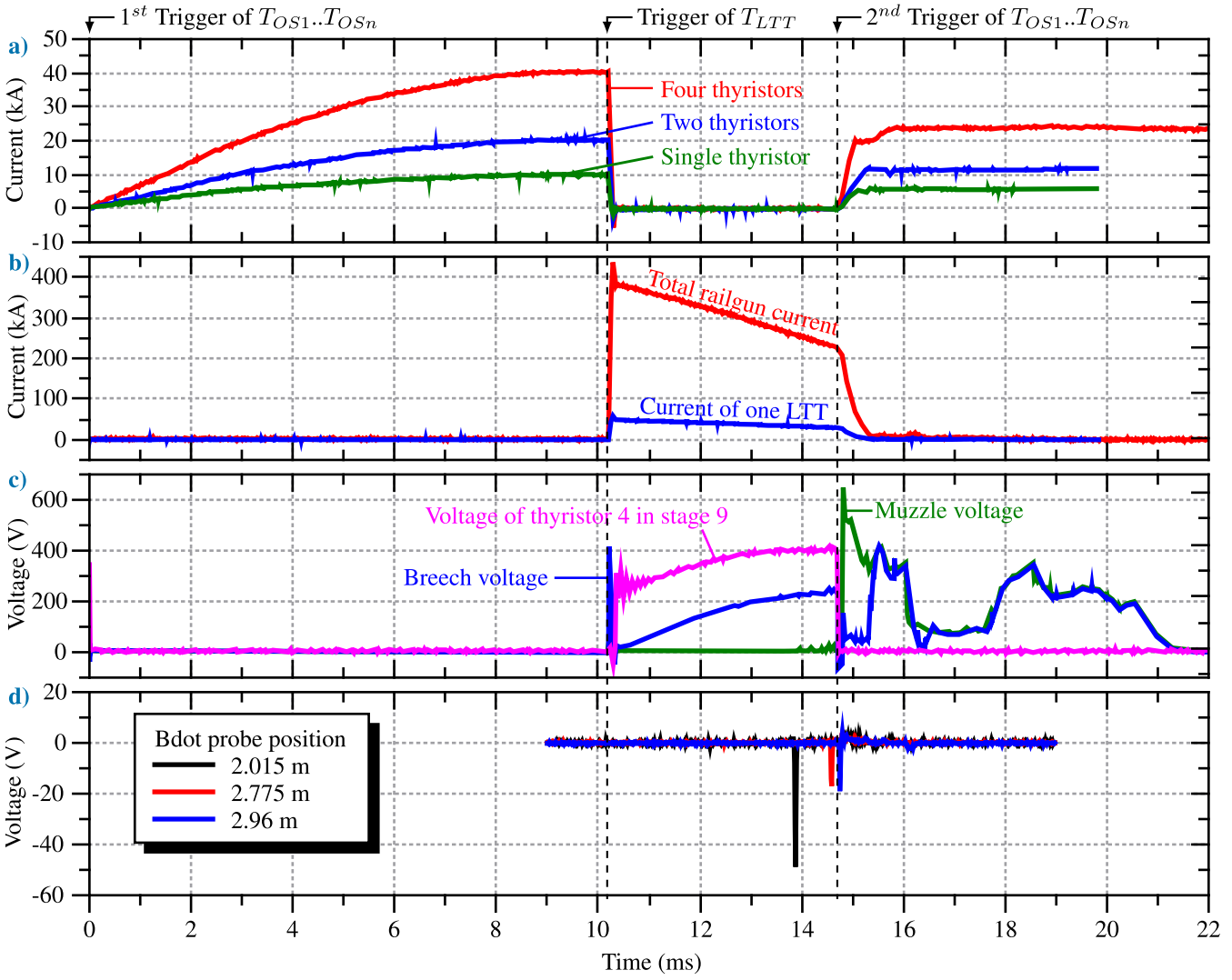

FIGURE 9. Measurements of the latest XRAM generator-supplied-railgun experiment with a stored energy of 842 kJ.

Thus, experiments with higher energy levels were not performed. In the following, only the experimental results of the latest railgun shot will be discussed in detail.

III. EXPERIMENTAL RESULTS AND ANALYSIS

A. RAILGUN SUPPLIED BY XRAM GENERATOR

1) STEP 1: CHARGING

The experiments started with the high voltage charging process of the 13 capacitor banks. This lasted several minutes and was therefore not recorded. The recordings start as can be seen in Fig. 9 a at t = 0 ms with the triggering of the opening switches. The trigger signal was given as soon as the capacitors reached a voltage of 7 kV. The inductive storage was then charged by the capacitors. The inductor current in the XRAM generator increased until 40 kA at t = 10.2 ms. The red curve (four thyristors) shows the total charging current which was measured in this case at the opening switch of stage 10. The blue and the green curve show the total current of two thyristors connected in parallel and the current of a single thyristor, respectively. The waveforms resemble the total current with half and a quarter of its amplitude, thus indicating a symmetric current distribution between the randomly measured thyristors of the opening switch assemblies.

2) STEP 2: RAILGUN SUPPLY

The LTTs of the main switch are triggered at t = 10.2 ms which initiates the discharge of the pre-charged counter-current capacitors ($C_{cc1} \ldots C_{ccn}$). The corresponding counter-current pulse can be recognized by the negative peak of the charging current of about −5 kA and by the positive railgun current peak of up to 435 kA. At the opening switches ($T_{OS1} \ldots T_{OS2}$), a hold-off interval of $\geq 70\,\mu$s has been measured (see Fig. 10). This is largely sufficient in order to insure a reliable turn-off of the thyristors which feature a recovery time of 20 μs. The voltage at the thyristor terminals, represented here by the voltage measurement at the

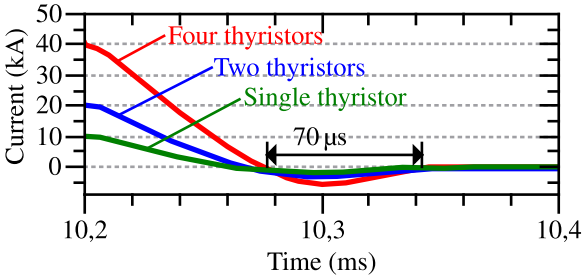

FIGURE 10. Zoom-in on the thyristor currents (see Fig. 9 a) at switching time.

4th thyristor of stage 9 (see Fig. 9 c), increases sharply to a very moderate amplitude of about 300 V, which is well below the voltage limit of the thyristor (1400 V). Some damped oscillations occur until t ≈ 10.5 ms due to the snubber elements. At this moment, they protect the thyristors against high voltage peaks. The XRAM output current, which is equal to the railgun current in Fig. 9 b, starts with the counter-current pulse and discharges approximately from 385 kA to 228 kA. The measured current at LTT 2 of the main switch shows in principle the same behavior but with one eighth of the amplitude. This means a symmetric current distribution between the LTT modules. Once the railgun current is switched on, the projectile in the accelerator begins to move. This can be seen by the rising voltage at the breech and at thyristor 4 of stage 9 (see Fig. 9 c). Note that both voltages are proportional to each other. The thyristor voltage is higher due to the additional voltage drop at the high current coaxial cables connecting the XRAM generator to the railgun breech.

3) STEP 3: TURNING-OFF THE RAILGUN CURRENT

The projectile reaches the end of the railgun at around 14.7 ms. This can be recognized by a sharp increase of the muzzle voltage (see Fig. 9 c). At this time, a current of 228 kA means that an energy of approximately 260 kJ is still stored in the coil. This energy can be either fed to a large muzzle arc or, as was demonstrated to some extent, used for the next charging cycle. As the energy for charging the inductor was insufficient for more than one shot, the demonstration was limited to switching the XRAM generator back to the charging state and to reduce the muzzle arc. A muzzle arc generates undesired heat, light and noise emissions and leads to increased wear at the railgun muzzle. Switching on the opening switches a second time after projectile launch results in a drastic current drop at the load and simultaneously a steep current rise at the charging circuit (see Fig. 9 a). The opening switch thyristors of the 10 stages were triggered at t = 14.7 ms just after the passage of the B-dot probe at 2.775 m (see Fig. 9 d). Successful switch-on can be recognized by the voltage drop from 400 V to 0 V at Th4 at stage 9. Shortly after, the projectile leaves the railgun bore and the muzzle voltage increases suddenly to approximately 650 V (see Fig.9 c) because the rail-to-rail contact is not made via the low-resistive armature but suddenly by a high-resistive plasma arc at the muzzle. According to U = L × dI/dt, this

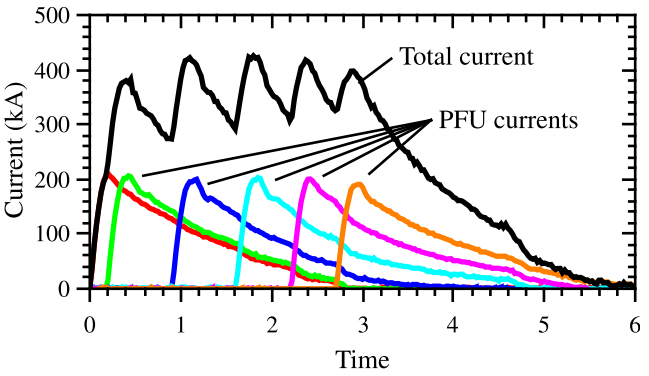

FIGURE 11. Railgun current generated by six PFUs.

voltage supports the current commutation from the load to the charging circuit of the XRAM generator. Thus, the railgun current decreases rapidly to zero after t = 15.3 ms and the current of the charging circuit increases at the same time to approximately 23 kA. An important aspect is that the current distribution of the parallel connected thyristors stays symmetric during the steep current rise. Otherwise, the dI/dt limit of a single device could be exceeded. After t = 15.3 ms, the LTT switches return to the blocking state as the railgun current is zero. Thus, the railgun is electrically separated from the rest of the circuit which leads to an undefined voltage potential for t > 15.3 ms. The average velocity was calculated to be 1064 m/s and 1121 m/s between the first and second B-dot locations and between the second and third B-dot location, respectively.

B. RAILGUN SUPPLIED BY CAPACITOR BANK

The railgun shot was compared to earlier RAFIRA shots where the railgun was directly supplied by capacitor banks. A shot with the same kind of projectile and an almost equal muzzle velocity of 1120 m/s was chosen. In this experiment, a single shot was supplied by 6 capacitor banks at a charging voltage of 10.25 kV. Each bank generates a current pulse with a maximum of about 200 kA. The superposition of those pulses at the railgun results in a total current pulse shape as given in Fig. 11. Fig. 12 shows additionally the velocity and muzzle voltage profiles during this shot. Note that the amplitude of the muzzle voltage was divided by 3 in order to fit it into this graph. The projectile left the bore at $t = 4.64$ ms.

IV. SHOT COMPARISON

A. GENERATOR CHARACTERISTICS

Table 5 lists the basic parameters of both experiments for a direct comparison. Note especially the difference of L and R. Thus, the time constant of the XRAM generator coil is more than one order of magnitude larger than L/R of the pulse forming coil of the capacitor bank.

B. PULSE SHAPE

Each RAFIRA capacitor bank is made from eight capacitors, a pulse forming coil, a trigatron (spark gaps with electrical

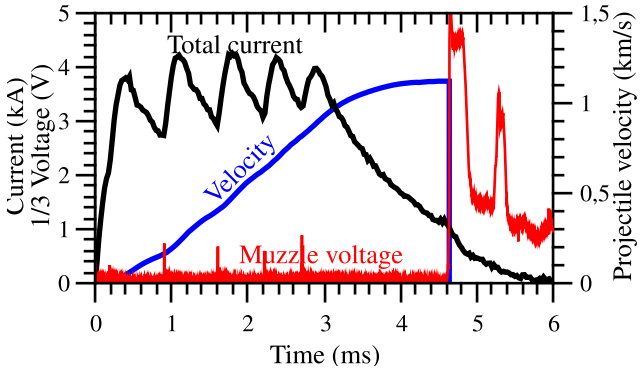

FIGURE 12. Measurements of railgun current, projectile velocity and muzzle velocity of a RAFIRA shot supplied with the capacitor banks.

TABLE 5. Comparison of experimental key values.

Pulsed power supply	XRAM generator	Capacitor bank
Pulse shape	Single pulse	Superposition of pulses
Charging impedance	1 mH / 6 mΩ	4 µH /280 µΩ
Discharging impedance	10 µH / 60 µΩ	4 µH / 280 µΩ
Max. current	433 kA	425 kA
Projectile mass	80.33 g	81.92 g
Stored energy	842 kJ	971 kJ
Muzzle velocity	1121 m/s	1120 m/s

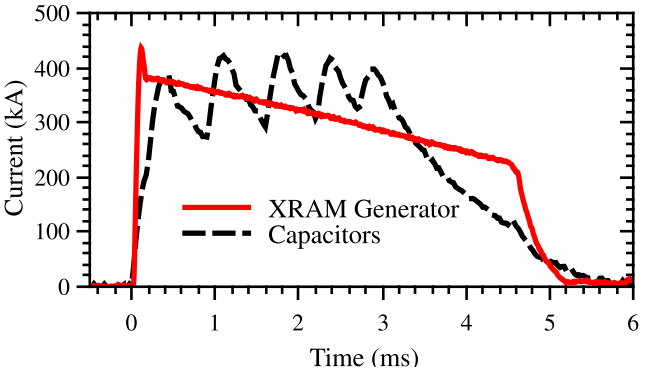

FIGURE 13. Comparison of current pulses.

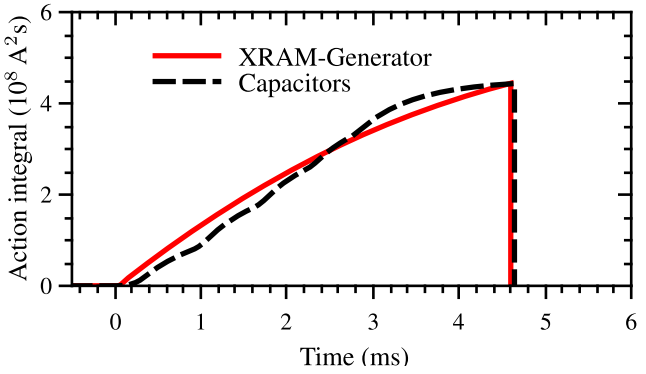

FIGURE 14. Comparison of action integrals.

trigger mechanism) and a crowbar diode assembly. The operating mechanism is as follows: After the Trigatron is switched on, the pre-charged capacitors discharge to the bank's pulse forming coil and the railgun at once as they are connected in a series connection. After the capacitor is discharged, the crowbar diodes, which are placed in parallel to the capacitors, become conductive and the capacitor is bypassed. From this moment, only the pulse forming inductor is supplying the railgun. Thus, a capacitor bank with pulse forming coils can be seen as an IPPS as well.

Several capacitor banks are connected in parallel to the railgun. Thus, each unit can be triggered independently from the others, allowing to form an arbitrary pulse shape. At the chosen experiment, the capacitors were discharged with a time delay that resulted in the approximation of a rectangular pulse shape. As result, the current pulse consists of the superposition of six single pulses with five local current peaks. This might be important with respect to the mechanical design of the railgun and the armature-rail contact as the electromagnetic forces are proportional to the square of the current. In case of the XRAM generator, all stages were switched simultaneously and one single pulse with a short spike (the counter-current pulse) was generated. Unlike the capacitor bank, it decays smoothly with an exponential slope defined by the time constant of the discharge circuit. Fig.13 shows the corresponding current pulses. Both current pulses last approximately 5 ms. The exit of the projectile occurs in both cases at about $t = 4.6$ ms. It can be detected by the sudden drop of the currents. In case of the capacitor bank, the remaining current in the rails is about 110 kA at this time. This current has to be as small as possible because it defines the residual energy in the inductance of the railgun and its cables, which is consumed by a muzzle flash. The latter is established during the exit of the armature and connects the two rail endings by a plasma. The remaining current of the XRAM generator during the muzzle exit is still more than 200 kA. It means that more inductive energy remains in the system after shot out. This is caused by the smaller current decay or higher discharge time constant, respectively, in case of the XRAM generator. On the other hand, it also means that the projectile experiences high forces until it reaches the muzzle. Fig. 14 shows the integration of the squared currents, the so-called action integrals of both experiments. Note that the action integral is directly proportional to the projectile velocity. Thus, it is a valid reproduction of the velocity profile (compare velocity in Fig. 12 with the capacitor curve in Fig. 14). In case of the capacitive PPS (CPPS), the action integral increases almost linearly with some bumps due to the time delayed triggering of the capacitor banks. After $t = 3.5$ ms, the curve asymptotically approaches the final value. In case of the XRAM generator, the curve increases smoothly with an exponential behavior before it reaches the same maximum value. This corresponds to the fact that the muzzle velocity of both experiments was the same.

After the shot-out of the projectile, the current decreases faster in case of the XRAM generator because the charging circuit was switched on again. Thus, the muzzle flash was kept small and the remaining inductive energy could have

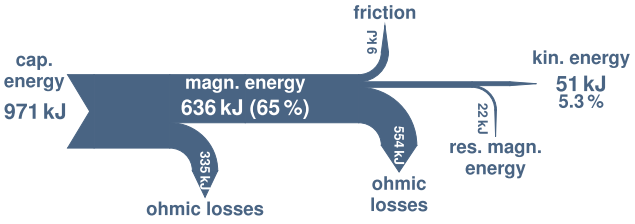

FIGURE 15. Energy flow of the classical RAFIRA experiment supplied by the capacitor banks.

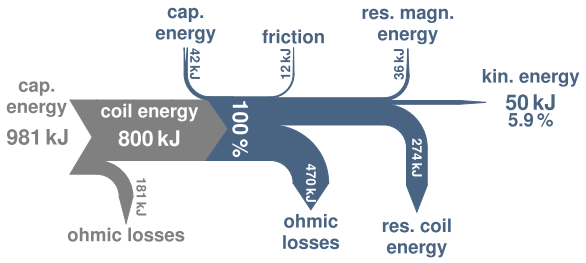

FIGURE 16. Energy flow of the RAFIRA experiment supplied by the XRAM generator.

been used again if the means for an additional charging process had been available. Unfortunately, this time, the energy was just dissipated in the resistance of the circuit.

C. EFFICIENCY OF THE ENERGY CHAINS

Finally, the energy chains were compared (see Figs. 15 & 16). Fig. 15 represents the energy flow from the capacitive stored energy at the beginning until the kinetic energy of the projectile during the classical railgun shot. In between, the energy is stored temporarily in the magnetic field of the circuit inductances (pulse forming inductance, cables and railgun). Energy is lost due to ohmic losses, friction and unused magnetic energy. The first ohmic losses occur until the current reaches its maximum (inductor charging). The other ohmic losses occur thereafter. The allocation of losses to individual components like coil, switches, cables and railgun was not possible due to insufficient measurement data. Residual magnetic energy remains in the system at the end of the shot and is dissipated in the muzzle flash. The conversion efficiency from capacitive to kinetic energy is 5.3%.

The corresponding Sankey diagram of the railgun shot with the XRAM generator as power supply is shown in Fig. 16. For the sake of completeness, the diagram starts with the charged capacitors. However, this first part is shown in gray as the efficiency analysis is based on the charged inductive storage. Thus, 800 kJ magnetic and 42 kJ capacitive energy of the counter-current capacitors are considered as 100 %. As before, a large part of the energy is lost due to friction, ohmic losses and magnetic energy which remains in the system after the muzzle exit of the projectile. This time, a distinction was made between the residual coil energy and the residual magnetic energy in the railgun and cables. Finally, the projectile has a kinetic energy of 50 kJ which results in a conversion efficiency of 5.9 %. This is slightly higher than with the capacitor bank. The efficiency can be improved to 9 % if the resuming coil energy of the last shot is assumed to be re-used. Thus, the coil needs to be re-charged only by 568 kJ.

V. DISCUSSION

The turn-off of a charging current of 40 kA by a semiconductor switch array was successful demonstrated. As far as the authors know, such current amplitudes were only achieved by mechanical or explosive opening switches until now. Furthermore, a railgun of a size which might be suitable for a future CIWS was supplied by an XRAM generator. However, experiments had to be stopped because the max. capacitor capacity and the switch voltage limit imposed a maximum inductive energy of 800 kJ which is 20 % below the goal of 1 MJ. This is a result of the fact that a capacitor bank was used instead of a low-voltage power supply like batteries. Hence, the charging time of the inductor was rather short. In the future, the charging time with a low-voltage source might take more time, which increases the action integral and therefore the thermal stress on the switches and the conductors remarkably. It also means a different dI/dt which might affect the current balancing between the switching components.

A higher action integral due to longer charging time would also impose more losses. As mentioned before, that the comparison in section IV-B is done by assuming charged short term storages (capacitor bank and inductive storage) and thus, the efficiency looks very advantageous for the XRAM generator. A theoretical comparison of the complete energy chain in [8] indicated a better overall efficiency for the capacitor bank. Further work with respect to fast and powerful coil and capacitor charging will be necessary in the future.

It has to be mentioned that the conversion efficiency of our experiments is quite small. However, this is not a show-stopper because the efficiency is proportional to the projectile velocity. Thus, railgun efficiencies up to 41% were demonstrated at more powerful experiments [36].

A long-term goal, as mentioned in the introduction, is the proof of IPPS compactness in order to evaluate the possibilities of system integration and mobile application of the railgun. Note in this respect, that the presented setup is still a breadboard installation which is not yet optimized for compactness (see Fig. 8). To answer the question if IPPS or CPPS are more suitable, it would be necessary to optimize the coil as mentioned in [50] and to use a purpose designed energy supply, counter-current capacitors and switches (LTTs). Furthermore, the complete energy chain needs to be compared. However, even then, a general comparison between IPPS and CPPS remains difficult as many factors (like application scenario, supply interface, installation constraints, segmentation, distance between PPS and load, cooling,..) influence the system size and might favor one or the other solution in different cases. Nonetheless, the energy density of the toroidal coil was 3.6 MJ/cm^3 during the last experiment which is only slightly better than a high-power dielectric capacitor but was not yet

used until its stress limits. It was already tested with a current of 50 kA, which means an energy density of 5.7 MJ/m^3. FEM simulations predict its mechanical limit at 10 MJ/m^3. See [50] for further details. The authors are confident that improved toroidal coil designs with additional mechanical support might reach 20 MJ/m^3 or more but suspect that thermal heating and not mechanical constraints will ultimately limit the energy density.

Another point to discuss is the counter-current pulse. In an ideal case, the railgun works best with a smooth rectangular (flat-top) current pulse. In case of the XRAM generator, the counter-current pulse represents a short and high current spike at the beginning of the supply pulse. Although it contributes little to the projectile acceleration, it generates high forces which need to be mechanically compensated. It did not provoke any problems in the present case as the forces stay far below the limits of the used railgun but it needs to be considered in future designs. It should be pointed out that the amplitude ratio of the discharge current to counter-current depends on the ratio between storage inductance and parasitic inductance. Thus, the counter-current peak was 113% of the discharge current amplitude. In previous experiments with smaller storage inductances, the excess was as high as 133% [65] or 145% [47]. The larger the system, the smaller the excess due to the counter-current pulse.

VI. CONCLUSION

As a continuation of the XRAM generator development at ISL, the new goal was a demonstrator with a stored energy of 1 MJ and its use as power supply for a medium caliber railgun. Its realization required the development and construction of an inductive storage and switches for a current greater than 40 kA. The coil was realized as toroidal copper coil with a total mass of 1 ton and a volume of 220 l. Switches were realized by thyristors and LTTs in a parallel connection. The former were applied as opening switches by turning them off with a counter-current pulse generated by additional capacitors. Current balancing between the single semiconductor devices was a challenge and required additional measures (see above). A stored energy of 842 kJ at a charging current of 40 kA were achieved at the final railgun experiment. Both values are new benchmarks at ISL and for XRAM generators with semiconductor switches in general. The maximum energy was limited by the voltage limit of the used components. Thus, the maximum capacitor voltage was 7 kV. A more suitable (low voltage) current source was not available. Thus, budget limitations and not technical reasons stopped us from reaching higher energy levels.

The energy density of the coil reached 3.6 MJ/m^3 in this experiments although the coil alone was already tested for 5.7 MJ/^{3} and the maximum energy density is estimated to be 10 MJ/m^3 [50].

The XRAM generator was successfully used to supply ISL railgun RAFIRA with a peak current of 400 kA. An 80 g projectile was successfully accelerated to 1120 m/s. The shot was compared with a classical RAFIRA shot from the past with very similar results. The XRAM showed a slightly better performance if the charging circuit of both, XRAM generator and capacitor bank, is not taken into consideration. The efficiency balance of the XRAM generator can be improved if the residual magnetic energy of the coil is used for another shot. This possibility was proven in principle by switching on the coil charging circuit a second time.

The new XRAM generator also showed a reduced peak-to-peak ratio between counter-current pulse and discharge pulse in comparison to small energy demonstrators of the past. This is important with respect to the mechanical compensation of electromagnetic forces.

No show-stopper has been faced in realizing the XRAM generator in the MJ-range although the semiconductor switches must be designed very carefully for each new design.

ACKNOWLEDGMENT

The authors acknowledge the help of all colleagues who helped with the preparation and execution of the experiments, especially Bernard Grasser.

REFERENCES

[1] X. Vavasseur (2020) *Eda Launches, 'PILUM,' Research Study on Electromagnetic Railguns*. Accessed: Aug. 18, 2020. [Online]. Available: https://www.navalnews.com/naval-news/2020/05/eda-launches-pilium-research-study-on-electromagnetic-railguns/

[2] S. J. Freedberg, Jr. (2017). *Navy Railgun Ramps up in Test Shots*. Accessed: Sep. 23, 2020. [Online]. Available: https://breakingdefense.com/2017/05/navy-railgun-ramps-up-in-test-shots/

[3] (2012). *Office of Naval Research*. Accessed: Jan. 23, 2014. [Online]. Available: https://www.onr.navy.mil

[4] J. Seidel. (2018). *China's Railgun Confirmed: Military 'Award' Reveals Electromagnetic Supergun Tested At Sea*. Accessed: Jun. 16, 2020. [Online]. Available: https://www.news.com.au/technology/innovation/chinas-supergun-nears-readiness/news-story/f3554a1cc140413ae16af7078f0e5cca

[5] Company Website. (2012). *Anadolu Yönlendirilmiş Enerji Technolojileri A. Ş.* [Online]. Available: https://www.yeteknoloji.com/en/corporate/

[6] S. Hundertmark and D. Lancelle, "A scenario for a future European shipboard Railgun," *IEEE Trans. Plasma Sci.*, vol. 43, no. 5, pp. 1194–1197, May 2015.

[7] J. Gallant, T. Vancaeyzeele, B. Lauwens, B. Wild, F. Alouahabi, and M. Schneider, "Design considerations for an electromagnetic railgun firing intelligent bursts to be used against antiship missiles," *IEEE Trans. Plasma Sci.*, vol. 43, no. 5, pp. 1179–1184, May 2015.

[8] O. Liebfried, S. Hundertmark, and P. Frings, "Inductive pulsed power supply for a railgun artillery system," *IEEE Trans. Plasma Sci.*, vol. 47, no. 5, pp. 2550–2555, May 2019.

[9] O. Liebfried, "Review of inductive pulsed power generators for railguns," *IEEE Trans. Plasma Sci.*, vol. 45, no. 7, pp. 1108–1114, Jul. 2017.

[10] X. Yu and X. Liu, "Overview of circuit topologies for inductive pulsed power supplies," *CES Trans. Electr. Mach. Syst.*, vol. 1, no. 3, pp. 265–272, Sep. 2017.

[11] D. Deis and I. McNab, "A laboratory demonstration electromagnetic launcher," *IEEE Trans. Magn.*, vol. 18, no. 1, pp. 16–22, Jan. 1982.

[12] R. A. Marshall and W. Ying, *Railguns: Their Science and Technology*. Beijing, China: China Machine Press, 2004.

[13] I. R. McNab, "Homopolar generators for electric guns," *IEEE Trans. Magn.*, vol. 33, no. 1, pp. 461–467, Jan. 1997.

[14] A. Pokryvailo, "Development of long-charge inductive storage systems at soreq NRC," in *Proc. IEEE Pulsed Power Conf.*, Monterey, CA, USA, Jun. 2005, pp. 100–103.

[15] Y. Aso and S. Yamada, "Current multiplier by inductive storage (CMIS) cooled by LN_2 and design of mega-ampere CMIS," *IEEE Trans. Plasma Sci.*, vol. 39, no. 1, pp. 247–250, Jan. 2011.

[16] A. Sitzman, D. Surls, and J. Mallick, "Stretch meat grinder: A novel circuit topology for reducing opening switch voltage stress," in *Proc. IEEE Pulsed Power Conf.*, Monterey, CA, USA, Jun. 2005, pp. 493–496.
[17] A. Sitzman, D. Surls, and J. Mallick, "Design, construction, and testing of an inductive pulsed-power supply for a small railgun," *IEEE Trans. Magn.*, vol. 43, no. 1, pp. 270–274, Jan. 2007.
[18] A. Sitzman, D. Surls, and J. Mallick, "Modification and testing of a battery-inductor repetitive pulsed power supply for a small railgun," in *Proc. 16th IEEE Int. Pulsed Power Conf.*, vol. 2, Albuquerque, NM, USA, Jun. 2007, pp. 1793–1798.
[19] A. Sitzman, "private communication," San Francisco, CA, USA, Jun. 2013.
[20] H. Sun, X. Yu, B. Li, P. Zhu, Z. Li, and H. He, "Meat grinder with ACC circuit: A novel circuit for inductive pulsed power supplies," *IEEE Trans. Plasma Sci.*, vol. 48, no. 2, pp. 566–570, Feb. 2020.
[21] X. Yu, H. Sun, X. Liu, J. Li, Z. Li, and H. He, "Design, construction, and testing of an 80-kJ and 2.4-MJ/m3 inductive pulsed power module for electromagnetic launchers," *IEEE Trans. Plasma Sci.*, vol. 48, no. 1, pp. 285–290, Jan. 2020.
[22] H. Li, Y. Wang, Y. Zhu, R. Wu, L. Dong, and K. Dou, "Design and testing of a high-temperature superconducting pulsed-power transformer," *IEEE Trans. Appl. Supercond.*, vol. 22, no. 2, Apr. 2012, Art. no. 5500205.
[23] R. Wu, Y. Wang, Z. Yan, W. Luo, and Z. Gui, "Design and experimental realization of a new pulsed power supply based on the energy transfer between two capacitors and an HTS air-core pulsed transformer," *IEEE Trans. Plasma Sci.*, vol. 41, no. 4, pp. 993–998, Apr. 2013.
[24] R. Wu, Y. Wang, Z. Yan, Z. He, and L. Wang, "Design and testing of a novel inductive pulsed power supply consisting of HTS pulse power transformer and ZnO-based nonlinear resistor," *IEEE Trans. Plasma Sci.*, vol. 41, no. 7, pp. 1781–1786, Jul. 2013.
[25] R. Wu, Y. Wang, Z. Yan, Z. He, and L. Wang, "Simulation and experimental investigation of an inductive pulsed power supply based on the head-to-tail series model of an HTS air-core pulsed transformer," *IEEE Trans. Appl. Supercond.*, vol. 23, no. 4, Aug. 2013, Art. no. 5701305.
[26] Y. He, Y. Wang, F. Lu, Z. He, and Z. Yan, "Analysis and exploiting of mutual coupling effect on inductive pulsed power supply consisting of multiple HTS pulse power transformers," *IEEE Trans. Appl. Supercond.*, vol. 27, no. 6, Sep. 2017, Art. no. 3602107.
[27] F. Lu, X. Nie, Y. Wang, W. Chen, and Z. Yan, "Influence of the mutual inductance between two HTSPPT modules on three discharge modes of superconducting pulsed power supply," *IEEE Trans. Plasma Sci.*, vol. 46, no. 8, pp. 2993–2998, Aug. 2018.
[28] F. Lu, Z. Yan, L. Liang, and Y. Wang, "Arrangement optimization of the superconducting pulsed power transformer of inductive pulsed power supply," *IEEE Trans. Appl. Supercond.*, vol. 29, no. 2, Mar. 2019, Art. no. 5500305.
[29] F. Lu, Y. Wang, X. Wang, X. Liao, Z. He, and Z. Yan, "Study on the collaborative discharge of a double superconducting pulsed power supply based on HTSPPT modules," *IEEE Trans. Appl. Supercond.*, vol. 28, no. 2, Mar. 2018, Art. no. 5700107.
[30] X. Zhang, Z. Li, H. Li, C. Zhang, and S. Liu, "A high-temperature superconducting pulsed-power supply circuit with ICCOS," *IEEE Trans. Plasma Sci.*, vol. 46, no. 11, pp. 4023–4027, Nov. 2018.
[31] X. Liang, H. Li, C. Zhang, Y. Zhang, Y. An, Z. Li, and X. Zuo, "An improved repetitive inductive pulsed power supply circuit with ICCOS technique," *IEEE Trans. Plasma Sci.*, vol. 48, no. 4, pp. 1082–1087, Apr. 2020.
[32] T. Zhang, H. Li, C. Zhang, Q. Wang, L. Zhai, Y. An, and Y. Chen, "Design and simulation of a multimodule superconducting inductive pulsed-power supply model for a railgun system," *IEEE Trans. Plasma Sci.*, vol. 47, no. 2, pp. 1352–1357, Feb. 2019.
[33] H. Li, Y. Wang, W. Chen, W. Luo, Z. Yan, and L. Wang, "Inductive pulsed power supply consisting of superconducting pulsed power transformers with Marx generator methodology," *IEEE Trans. Appl. Supercond.*, vol. 22, no. 5, Oct. 2012, Art. no. 5501105.
[34] B. Wang. (2016). *Shipping Containers Full of Capacitors Will Enable Flexible Railgun Designs for Shipboard and Fixed or Mobile Land Based Railguns*. Accessed: Jun. 19, 2020. [Online]. Available: https://www.nextbigfuture.com/2016/05/shipping-containers-full-of-capacitors.html
[35] E. Spahn, G. Buderer, and F. Hatterer, "Compact 50 kJ pulse forming unit, switched by semiconductors," *IEEE Trans. Magn.*, vol. 31, no. 1, pp. 78–83, Jan. 1995.
[36] S. Hundertmark, G. Vincent, D. Simicic, and M. Schneider, "Increasing launch efficiency with the PEGASUS launcher," *IEEE Trans. Plasma Sci.*, vol. 45, no. 7, pp. 1607–1613, Jul. 2017.
[37] S. Scharnholz, V. Brommer, G. Buderer, and E. Spahn, "High-power MOSFETs and fast-switching thyristors utilized as opening switches for inductive storage systems," *IEEE Trans. Magn.*, vol. 39, no. 1, pp. 437–441, Jan. 2003.
[38] S. Scharnholz, R. Schneider, E. Spahn, A. Welleman, and S. Gekenidis, "Investigation of IGBT-devices for pulsed power applications," in *14th IEEE Int. Pulsed Power Conf. Dig. Tech. Papers.*, vol. 1, Dallas, TX, USA, Jun. 2003, pp. 349–352.
[39] P. Dedie, V. Brommer, and S. Scharnholz, "ICCOS countercurrent-thyristor high-power opening switch for currents up to 28 kA," *IEEE Trans. Magn.*, vol. 45, no. 1, pp. 536–539, Jan. 2009.
[40] E. Van Dijk and P. Van Gelder, "A resonant series counterpulse technique for high current opening switches," *IEEE Trans. Magn.*, vol. 31, no. 1, pp. 84–89, Jan. 1995.
[41] E. van Dijk and P. van Gelder, "100 kA test results of the 1 MA resonant series counterpulse opening switch system," in *10th IEEE Int. Pulsed Power Conf. Dig. Tech. Papers*, vol. 2, Albuquerque, NM, USA, Jul. 1995, pp. 1303–1308.
[42] E. van Dijk, "Experimental results obtained with the 1 MA resonant series counterpulse opening switch system, developed at TNO," in *11th IEEE Int. Pulsed Power Conf. Dig. Tech. Papers*, vol. 1, Chicago, IL, USA, Jun. 1997, pp. 287–292.
[43] W. Koch, "Ein induktiver Stoßstromgenerator für Hochstromexperimente," German Federal Ministry for Scientific Research [Bundesministerium für wiss. Forschung], Tech. Rep. BMwF-FB K 67-35, 1967.
[44] P. Dedie and V. Brommer, "Wire explosion fed by a 32-kJ XRAM generator switched by semiconductor elements," in *Proc. IET Eur. Conf. Eur. Pulsed Power Incorporating CERN Klystron Modulator Workshop*, Sep. 2009, p. 33, doi: 10.1049/cp.2009.1664.
[45] P. Dedie, V. Brommer, and S. Scharnholz, "Experimental realization of an eight-stage XRAM generator based on ICCOS semiconductor opening switches, fed by a magnetodynamic storage system," *IEEE Trans. Magn.*, vol. 45, no. 1, pp. 266–271, Jan. 2009.
[46] P. Dedie, V. Brommer, and S. Scharnholz, "Twenty-stage toroidal XRAM generator switched by countercurrent thyristors," *IEEE Trans. Plasma Sci.*, vol. 39, no. 1, pp. 263–267, Jan. 2011.
[47] O. Liebfried and V. Brommer, "A four-stage XRAM generator as inductive pulsed power supply for a small-caliber railgun," *IEEE Trans. Plasma Sci.*, vol. 41, no. 10, pp. 2805–2809, Oct. 2013.
[48] E. Spahn, K. Sterzelmeier, C. Gauthier-Blum, V. Brommer, L. Sinniger, and B. Grasser, "50 kJ ultra-compact pulsed-power supply unit for active protection launcher systems," in *Proc. 14th Symp. Electromagn. Launch Technol.*, Jun. 2008, pp. 1–5, doi: 10.1109/ELT.2008.13.
[49] O. Liebfried, V. Brommer, and S. Scharnholz, "Development of XRAM generators as inductive power sources for very high current pulses," in *Proc. 19th IEEE Pulsed Power Conf. (PPC)*, San Francisco, CA, USA, Jun. 2013, pp. 1–6, doi: 10.1109/PPC.2013.6627504.
[50] O. Liebfried, V. Brommer, H. Scharf, M. Schacherer, and P. Frings, "Modular toroidal copper coil for the investigation of inductive pulsed power generators in the MJ-range," *IEEE Trans. Appl. Supercond.*, vol. 30, no. 4, pp. 1–6, Jun. 2020, doi: 10.1109/TASC.2020.2971205.
[51] *Phase Control Thyristor T2563NH*, Datasheet, Infineon, Neubiberg, Germany, 2011.
[52] V. Brommer and O. Liebfried, "Parallelizing thyristors in a switch assembly for an inductive pulsed power generator," in *Proc. Workshop Switches Pulsed Power Appl.*, Mar. 2020.
[53] B. Wild, F. Alouahabi, D. Simicic, M. Schneider, and R. Hoffman, "A comparison of C-shaped and brush armature performance," *IEEE Trans. Plasma Sci.*, vol. 45, no. 7, pp. 1227–1233, Jul. 2017.
[54] O. Liebfried, M. Schneider, T. Stankevic, S. Balevicius, and N. Zurauskiene, "Velocity-induced current profiles inside the rails of an electric launcher," *IEEE Trans. Plasma Sci.*, vol. 41, no. 5, pp. 1520–1525, May 2013.
[55] D. A. Ward and J. L. T. Exon, "Using Rogowski coils for transient current measurements," *Eng. Sci. Educ. J.*, vol. 2, no. 3, pp. 105–113, Jun. 1993.
[56] S. E. Nyholm, P. Appelgren, T. Hurtig, and T. Hultman, "Design and calibration of Rogowski current probes," FOI–Swedish Defence Research Agency, Weapons and Protection, SE-147 25 Tumba, Tech. Rep. ISSN 1650-1942, Mar. 2002.
[57] S. Tumanski, "Induction coil sensors—A review," *Meas. Sci. Technol.*, vol. 18, no. 3, pp. R31–R46, Jan. 2007, doi: 10.1088/0957-0233/18/3/r01.

[58] N. D. Clements, "Hybrid integration for Rogowski coils and B-dot probes," in *Proc. 6th Int. Symp. Electromagn. Launch Techn.*, Austin, TX, USA, Apr. 1992.
[59] J. Wey, D. Eckenfels, C. Gauthier, and R. Charon, "High accuracy measurements on railguns," *IEEE Trans. Magn.*, vol. 31, no. 1, pp. 764–769, Jan. 1995.
[60] PEMUK, Power Electronics Measurements Ltd. (2010). *Datasheet 7CWT 0605*. Accessed: Nov. 11, 2010. [Online]. Available: https://www.pemuk.com/pdf/cmt1110.pdf
[61] Y. A. Dreizin and J. P. Barber, "On the origins of muzzle voltage," *IEEE Trans. Magn.*, vol. 31, no. 1, pp. 582–586, Jan. 1995.
[62] J. V. Parker, "Experimental observation of the rail resistance contribution to muzzle voltage [in railguns]," *IEEE Trans. Magn.*, vol. 35, no. 1, pp. 437–441, Jan. 1999.
[63] *Data Sheet High Voltage Probe Tektronix P6015A*, Tektronix, Beaverton, OR, USA, 1990.
[64] M. Schneider, D. Eckenfels, and S. Nezirevic, "Doppler-radar: A possibility to monitor projectile dynamics in railguns," *IEEE Trans. Magn.*, vol. 39, no. 1, pp. 183–187, Jan. 2003.
[65] P. Dedie, V. Brommer, and S. Scharnholz, "Twenty-stage toroidal XRAM generator switched by countercurrent thyristors," *IEEE Trans. Plasma Sci.*, vol. 39, no. 1, pp. 263–267, Jan. 2011.

OLIVER LIEBFRIED was born in Bottrop, Germany, in 1980. He received the Dipl.Ing.(FH) degree in electrical engineering and the M.Eng. degree in energy system technology from the Gelsenkirchen University of Applied Sciences, Gelsenkirchen, Germany, in 2004 and 2006, respectively, and the Ph.D. degree from Vilnius Gediminas Technical University, Vilnius, Lithuania, in 2011.

As Ph.D. student, he was with the State Research Institute Center for Physical Sciences and Technology, Vilnius, and the French-German Research Institute of Saint-Louis, France, where he has been a Research Scientist for pulsed power supplies for electromagnetic launchers, since 2011. His research interests include energy storages (batteries, capacitors, and inductors), switches (semiconductor switches and gas switches), converter topologies (HV charger and XRAM generator), electromagnetic accelerators, and dedicated metrology. He is an Executive Board Member of the International Society on Pulsed Power Applications e.V. (ISP).

Dr. Liebfried received the Award for outstanding young researchers at the Euro-Asian Pulsed-Power Conference, Chengdu, 2006.

VOLKER BROMMER was born in Germany, in March 1970. He received the Diploma degree in electrical energy technology from the Karlsruhe University of Applied Sciences, Karlsruhe, Germany, in 1998.

He joined the French-German Research Institute of Saint-Louis, France, in 1999. Since then, he has been with its Pulsed Power Group, specialized in high-power electronics and semiconductor switches.